

# Effect of Co Doping on the Elastocaloric Effect of Ni-Mn-Ga-Co Alloy

Haixu Qin<sup>1</sup>, Youping Zheng<sup>1</sup>, Liu Yang<sup>1</sup>, Sib0 Sun<sup>1\*</sup>, and Zhiyong Gao<sup>2\*</sup>

<sup>1</sup>Pangang Group Research Institute, Chengdu Advanced Metal Materials Industry Technology Research Institute, Titanium Metal Technology Department, Chengdu, 610000

<sup>2</sup>Science and Technology on Materials Performance Evaluation in Space Environment Laboratory, School of Materials Science and Engineering, Harbin Institute of Technology, Harbin, 150001, China

(Received 14 December 2022, Received in final form 11 August 2023, Accepted 18 August 2023)

Large latent heat is produced in the stress-induced martensitic phase transition process of Ni-Mn-Ga-based materials, i.e., elastocaloric effect. That makes such materials show tremendous potential for solid-state refrigeration which is identified as one of the most promising non-vapor-compression cooling devices. However, the still low refrigeration ability of these materials restricts further commercially promoting of solid-state refrigeration. In this work, we adjusted the Co content to regulate the elastocaloric effect for the Ni<sub>51.5</sub>Mn<sub>25</sub>Ga<sub>23</sub>Co<sub>0.5</sub>. According to the results, the transformation strain and ratio of loading stress/transformation temperature ( $d\sigma/dT$ ) were increased by replacing the Ni atoms with a little more Co, leading to an improvement of the stress-induced transformation entropy-change  $\Delta S_{\sigma}$ . As a result, a huge  $\Delta S_{\sigma}$  of 45.0 J Kg<sup>-1</sup>K<sup>-1</sup> is achieved in Ni<sub>50</sub>Mn<sub>25</sub>Ga<sub>23</sub>Co<sub>1</sub> alloy.

**Keywords :** Ni-Mn-Ga, Co doping, elastocaloric effect, transformation entropy-change

## 1. Introduction

Refrigeration, one of the indispensable technologies in our modern society, plays an irreplaceable effect in numerous fields, such as pharmaceutical refrigerators, food preservation, indoor temperature control, etc. However, the current refrigeration technologies based on vapor compression discharge environmentally harmful greenhouse gases and is harmful to the human living environment [1, 2]. Elastocaloric cooling induced by uniaxial stress has been deemed the most promising candidate to attain this goal of eco-friendly cooling technology proposed by the US Department of Energy [3, 4]. The elastocaloric performance of one material is mainly determined by the entropy-change  $\Delta S$  and the adiabatic temperature change  $\Delta T_{ad}$  achieved in the transformation process [5, 6].

Recently, the elastocaloric effect has been extensively studied in shape memory alloys (SMAs) due to their large latent heat release/absorption associated with the stress-induced martensitic transformation process [7-10], Giant  $\Delta T_{ad}$  have been reported in various SMAs, such as

NiTiCu ~ 25.3 K [11], NiTi ~ 25 K [12], CuZnAl ~ 14.2 K [13], and CuAlMn ~ 13 K [14]. Nevertheless, the large driving force to induce the martensitic transformation restricts their further application in solid-refrigeration or micro-refrigeration [15]. Hence, the Ni-Mn-based magnetic-field driving shape memory alloys with low driving force have become a more powerful candidate. Meanwhile, these alloys also exhibit considerable magnetocaloric effect [16], meaning that the solid-state refrigeration made of them is hopefully driven by multi-field. The overlapping of these two caloric effects has been proven feasible in Ni-Mn-Ga-based alloys. Unlike the Ni-Mn-In, Ni-Mn-Sn, and Ni-Mn-Sb, the Ni-Mn-Ga exhibits magnetic and structural entropy changes with the sign [17]. That makes them most controversial in the Ni-Mn-based materials system.

The elastocaloric properties presented obvious orientation in the Ni-Mn-Ga-based alloys. Hence, the previous studies were committed to fabricating the single crystals (SC) or directionally solidified (DS) ingots, obtaining a decent  $\Delta T$  of about 10.0 K [17-19]. However, the preparation process is high-cost and inefficient. Hence, in this work, the polycrystalline Ni<sub>51.5</sub>Mn<sub>25</sub>Ga<sub>23</sub>Co<sub>0.5</sub> alloys are directly prepared by a simple arc-melting method. Meanwhile, we replace Ni with more Co, which could

©The Korean Magnetism Society. All rights reserved.

\*Corresponding author: Tel: +86-18846928309

e-mail: hit\_qinhaixu@163.com

change the transformation temperature and increase the lattice difference between the martensite and austenite. As a result, the transformation strain, as well as the  $d\sigma/dT$ , is significantly improved, thus leading to an enlarged transformation entropy change.

## 2. Experimental Section

Polycrystalline samples of Ni-Mn-Ga-Co alloys were prepared by arc melting the constituent elements (99.99 %) in an argon atmosphere. Then, the obtained ingots were annealed for 12 h at 1173 K under a vacuum environment followed by quenched in ice water. The strain induced by transformation was calculated from the  $\epsilon$ - $T$  curves measured by the Dynamic Mechanical Analysis (DMAQ800) in the compressive model, the sample size is  $\phi 1 \times 1.5$  mm and measured under a constant load of 8, 10, 13, 15, 18 MPa.

## 3. Results and Discussion

Fig. 1(a) shows the temperature-dependent strains  $\epsilon$  ( $\epsilon$ - $T$

curves) under different loads of the  $\text{Ni}_{51.5}\text{Mn}_{25}\text{Ga}_{23}\text{Co}_{0.5}$  alloys. Under the same loading, the  $\epsilon$  first presents a slight decline with the measuring temperature decreasing. Then, as the temperature decreases to a little higher than the transformation temperature, the applied stress could induce the austenite phases to transform into martensite phases, leading to the strain being sharply increased. Then, with the temperature further increasing, the transformation is finished, and the applied loading forces the strain continuously increase. Fig. 1(b)-(c) shows the  $\epsilon$ - $T$  curves of  $\text{Ni}_{51.5-x}\text{Mn}_{25}\text{Ga}_{23}\text{Co}_{0.5+x}$  ( $x = 0.5, 1.5, 2.5$ ). It can be observed that increasing the Co content doesn't change the characteristic of the  $\epsilon$ - $T$  curves, still reflecting typical martensite transformation features. Nevertheless, martensite transformation initiating temperature varies with the Co content.

The transformation strain could be obtained from the  $\epsilon$ - $T$  curves, which is shown in Fig. 2. All samples exhibit a positive correlation relation between the transformation strain  $\epsilon$  and applied stress  $\sigma$ , corresponding with rules that higher stress means a higher degree of phase transition completion. With the Co content increasing, the trans-

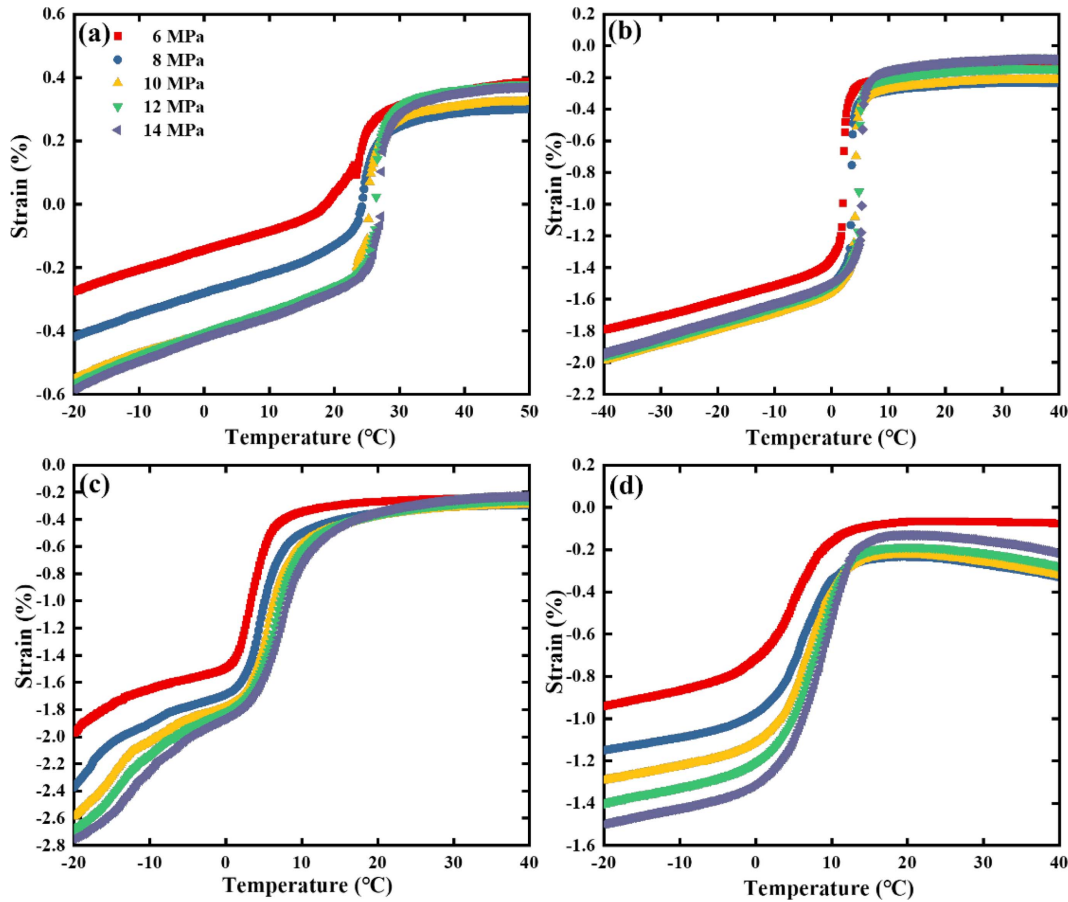


**Fig. 1.** (Color online) Temperature-dependent strains under different loading of 6, 8, 10, 12, and 14 MPa for  $\text{Ni}_{51.5-x}\text{Mn}_{25}\text{Ga}_{23}\text{Co}_{0.5+x}$ . (a)  $x = 0$ , (b)  $x = 0.5$ , (c)  $x = 1.5$ , (d)  $x = 2.5$ .

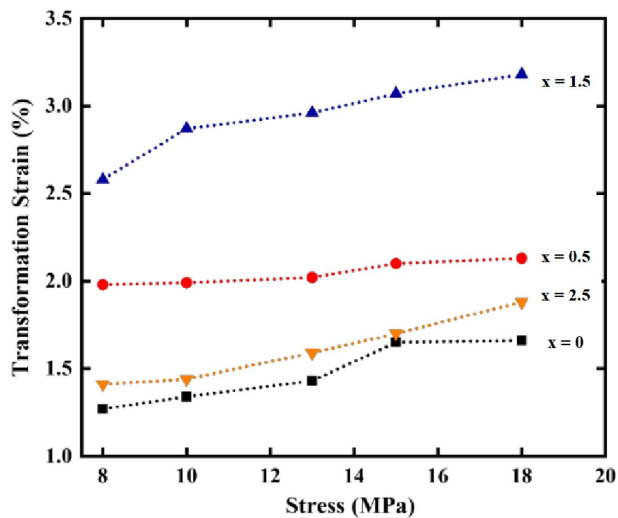


Fig. 2. (Color online) The testing stress dependence of the transformation strain for  $\text{Ni}_{51.5-x}\text{Mn}_{25}\text{Ga}_{23}\text{Co}_{0.5+x}$  alloys.

formation strain increases first and then decreases. Taking the loading of 8 MPa as an example, the transformation strain firstly increases from 1.27 % up to 2.58 % with the  $x$  increasing from 0 at.% up to 1.5 at.% and then decreases when Co content further increases. The final decline might be due to the 3 at.% Co has met its solution limit in Ni-Mn-Ga alloy, which leads to chaotic atom arrangement and extra second phases' occurrence. Ultimately, the  $\varepsilon$  reaches the maximum value of 3.18 % under the  $\sigma$  of 18 MPa in the  $\text{Ni}_{50}\text{Mn}_{25}\text{Ga}_{23}\text{Co}_2$ , much higher than the  $\text{Ni}_{51.5}\text{Mn}_{25}\text{Ga}_{23}\text{Co}_{0.5}$ . It can be concluded that enlarging the Co content could increase the lattice difference between the austenite and martensite phases in the trans-

formation process, thus leading to a huge transformation strain.

Fig. 3(a) shows the stress-dependent onset temperature of martensite transformation  $M_s$ . The  $M_s$  presents an upward tendency with the  $\sigma$  rising, due to that uniaxial stress applying could facilitate the martensite transformation. Under the same loading, the  $M_s$  decreases first and then increases with the Co content increasing. A minimum value of 6.01 °C is obtained under loading stress of 8 MPa as the Co is 1.0 at.%. In addition, the slope of the  $\sigma - T_M$  curves also varies with the Co content, meaning the  $d\sigma/dT$  is also changed. Shown in Fig. 3(b), the Co content dependent  $d\sigma/dT$  curves present a peaking effect, the  $d\sigma/dT$  reaches its peak value by adding 0.5 at.% Co.

According to the Maxwell relation (equation (1)) [8], we can calculate the stress-induced entropy  $\Delta S_\sigma$  change during the stress-induced martensitic transformation process. Fig. 4 presents the temperature-dependent  $\Delta S_\sigma$  with different loading. Similar to the relation between the transformation strain and the loading stress, higher  $\Delta S_\sigma$  is also obtained with larger loading. From equation (1), the  $\Delta S_\sigma$  is directly related to the transformation strain and the  $d\sigma/dT$  which are both increased by adding a tiny amount of Co content of 0.5 at.%. Hence, the  $\text{Ni}_{50}\text{Mn}_{25}\text{Ga}_{23}\text{Co}_1$  possesses the highest  $\Delta S_\sigma$  of 45.0  $\text{JK}^{-1}\text{K}^{-1}$ , two times higher than the  $\Delta S_\sigma$  of  $\text{Ni}_{51.5}\text{Mn}_{25}\text{Ga}_{23}\text{Co}_{0.5}$ . Even compared to the  $\Delta S_\sigma$  reported in other Ni-Mn-based alloys, this value still stays in the leading position, as shown in Fig. 5. Moreover, the driving stress corresponding to the maximum  $\Delta S_\sigma$  is only 18 MPa for our Co-doped sample, much lower than that used in the other work, which is in favor of the practical application.

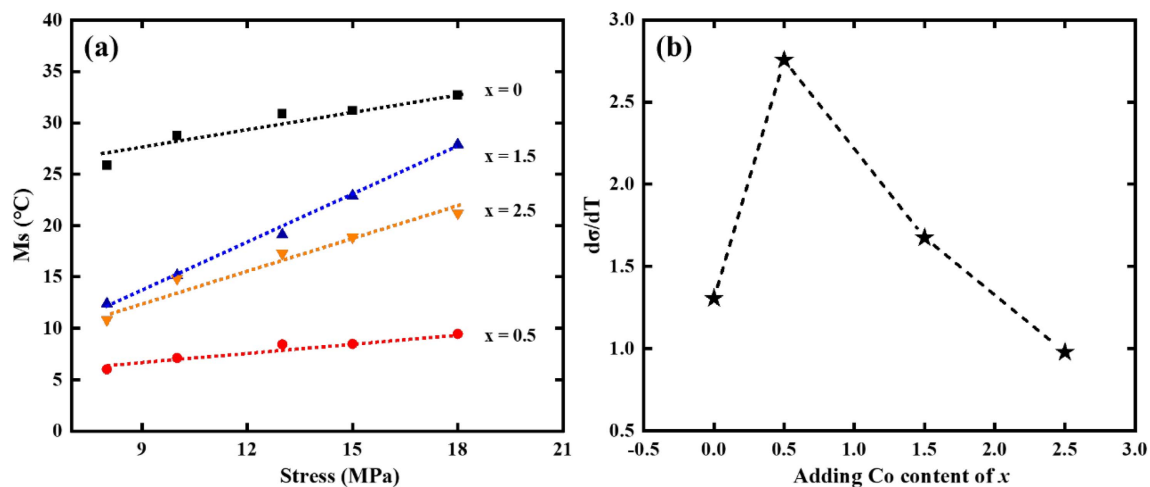
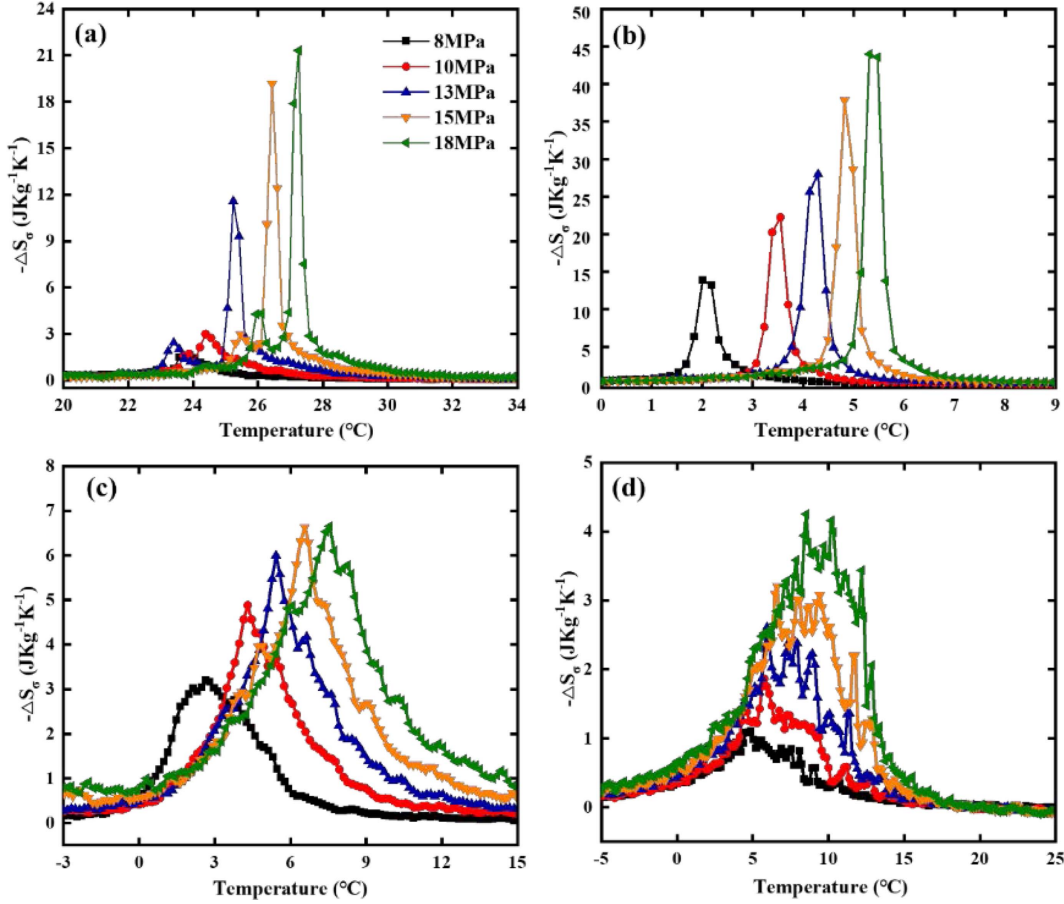
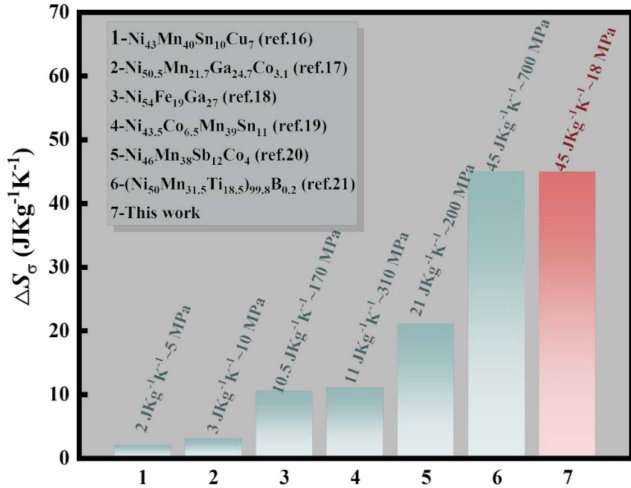


Fig. 3. (Color online) (a) Stress-dependent martensite transformation starting temperature and (b)  $d\sigma/dT$  of  $\text{Ni}_{51.5-x}\text{Mn}_{25}\text{Ga}_{23}\text{Co}_{0.5+x}$  alloys.



**Fig. 4.** (Color online) Temperature-dependent  $\Delta S_\sigma$  under different loading of 6, 8, 10, 12, and 14 MPa for  $\text{Ni}_{52-x}\text{Mn}_{25}\text{Ga}_{23}\text{Co}_x$ . (a)  $x = 0.5$ , (b)  $x = 1$ , (c)  $x = 2$ , (d)  $x = 3$ .



**Fig. 5.** (Color online) Comparison of  $\Delta S_\sigma$  between our Co-doped sample and other reported Ni-Mn-based alloys.

$$\Delta S_\sigma = v_0 \int_0^\sigma \left( \frac{\partial \varepsilon}{\partial T} \right)_\sigma d\sigma \quad (1)$$

Where  $v_0$  is the specific volume,  $\varepsilon$  is the applied stress, and  $T$  is the absolute temperature.

## 4. Conclusions

Substituting the Ni atoms with Co atoms in Ni-Mn-Ga alloys could manipulate the transformation temperature and the lattice difference between the austenite and martensite phases, as well as the transformation strain and  $d\sigma/dT$ . For the  $\text{Ni}_{50}\text{Mn}_{25}\text{Ga}_{23}\text{Co}_1$  sample, the transformation strain is significantly increased accompanied by the enlarged lattice difference between martensite and austenite. Meanwhile, the  $d\sigma/dT$  is also raised. Taken together, a huge  $\Delta S_\sigma$  of  $45.0 \text{ JKg}^{-1}\text{K}^{-1}$  is obtained, which makes this material show great potential for solid-state refrigeration.

## References

- [1] D. Matsunami, A. Fujita, K. Takenaka, and M. Kano, *Nat Mater* **14**, 73 (2015).
- [2] D. Cong, W. Xiong, A. Planes, Y. Ren, L. Manosa, P.

- Cao, Z. Nie, X. Sun, Z. Yang, X. Hong, and Y. Wang, *Phys. Rev. Lett.* **122**, 255703 (2019).
- [3] Energy savings potential and RD&D opportunities for non-vapor-compression HVAC technologies, Report of the U.S. Department of Energy, 2014, <https://energy.gov/eere/buildings/downloads/non-vapor-compression-hvac-technologies-report>.
- [4] B. Li, S. Li, B. Yang, H. Zhong, Z. Liu, and D. Li, *Journal of Alloys and Compounds* **936**, 168310 (2023).
- [5] Y. Xiao, W. Sun, J. Liu, X. Zhong, Z. Liu, M. Lu, K. Long, and H. Zhang, *Materials Letters* **251**, 1 (2019).
- [6] Y. Feng, X. Yuan, M. Zhou, and L. Gao, *Journal of Alloys and Compounds* **944**, 169143 (2023).
- [7] J. Tušek, K. Engelbrecht, D. Eriksen, S. Dall’Olio, J. Tušek, and N. Pryds, *Nature Energy* **1** (2016).
- [8] E. Bonnot, R. Romero, L. Manosa, E. Vives, and A. Planes, *Phys. Rev. Lett.* **100**, 125901 (2008).
- [9] X. Zhu, M. Qian, X. Zhang, S. Zhong, Z. Jia, R. Zhang, A. Li, and L. Geng, *Journal of Alloys and Compounds* **956**, 170291 (2023).
- [10] F. Xu, C. Zhu, J. Wang, F. Luo, X. Zhu, J. Xu, S. Chen, J. Wang, G. Ma, F. Chen, Y. Kuang, J. He, and Z. Sun, *Journal of Alloys and Compounds* **960**, 170768 (2023).
- [11] H. Chen, F. Xiao, X. Liang, Z. Li, Z. Li, X. Jin, and T. Fukuda, *Acta Materialia* **177**, 169 (2019).
- [12] J. Cui, Y. Wu, J. Muehlbauer, Y. Hwang, R. Radermacher, S. Fackler, M. Wuttig, and I. Takeuchi, *Applied Physics Letters* **101**, 073904 (2012).
- [13] Y. Wu, E. Ertekin, and H. Sehitoglu, *Acta Materialia* **135**, 158 (2017).
- [14] S. Xu, H.-Y. Huang, J. Xie, S. Takekawa, X. Xu, T. Omori, and R. Kainuma, *APL Materials* **4**, 106106 (2016).
- [15] W. Sun, J. Liu, B. Lu, Y. Li, and A. Yan, *Scripta Materialia* **114**, 1 (2016).
- [16] C. Yu, T. Chen, H. Yin, G. Kang, and D. Fang, *International Journal of Solids and Structures* **191-192**, 509 (2020).
- [17] J. Wang, Q. Yu, K. Xu, C. Zhang, Y. Wu, and C. Jiang, *Scripta Materialia* **130**, 148 (2017).
- [18] D. Li, Z. Li, J. Yang, Z. Li, B. Yang, H. Yan, D. Wang, L. Hou, X. Li, Y. Zhang, C. Esling, X. Zhao, and L. Zuo, *Scripta Materialia* **163**, 116 (2019).
- [19] D. Li, X. Zhang, G. Zhang, Z. Li, B. Yang, H. Yan, D. Wang, X. Zhao, and L. Zuo, *Applied Physics Letters* **118**, 213903 (2021).